J Mater Sci (2008) 43:4208–4214
DOI 10.1007/s10853-008-2606-1

Effect of sensitization heat treatment on properties of Al–Mg alloy AA5083-H116

I. N. A. Oguocha · O. J. Adigun · S. Yannacopoulos

Received: 1 July 2007 / Accepted: 17 March 2008 / Published online: 10 April 2008

Abstract Al–Mg alloy AA5083 is a sheet and plate alloy used mainly for marine application as well as for structural components in transportation and military applications. The strength is derived from solid solution strengthening and strain hardening. The properties of as-received and sensitized samples of AA5083-H116 were investigated using microhardness measurements, tensile testing, optical microscopy, Scanning Electron Microscopy (SEM), Energy Dispersive X-ray Spectroscopy (EDS), and Nitric Acid Mass Loss Test (NAMLT). The results show that both chemical and mechanical properties of the alloy decreased with increasing sensitization temperature and time. The deterioration in chemical property, which was measured in terms of the level of susceptibility to Intergranular Corrosion (IGC), is attributed to grain boundary precipitation of magnesium-rich particles. The loss in tensile and hardness properties is attributed to softening caused partly by decrease in Mg solute solid solution concentration with increasing sensitization time and temperature and partly by recrystallization at elevated temperatures.

Introduction

The need to reduce fuel consumption in transportation vehicles has generated strong interest in weight reduction through the use of strong, light-weight materials in their construction. Non-heat treatable wrought Al–Mg (5xxx series) alloys are the choice materials for components that require moderate strength, formability, weldability, and excellent atmospheric corrosion resistance. Nevertheless, Al–Mg alloys containing more than 3 wt.% Mg are susceptible to both Intergranular Corrosion (IGC) and Stress Corrosion Cracking (SCC) when exposed to elevated temperatures ($\geq$50 °C) in corrosive environments for sufficient length of time [1]. The extent of IGC susceptibility is a function of the corrodent, material chemistry, and fabrication and thermal process [2]. Consequently, the industrial application of these alloys is limited to low temperatures.

Several investigators have studied the IGC and SCC susceptibility of AA5xxx alloys and the general consensus is that it is caused by preferential precipitation of magnesium-rich particle, the β phase (Al_2Mg_3), along the grain boundaries [1–21]. Davenport et al. [3] investigated the IGC and SCC of sensitized AA5182 using Atomic Force Microscopy (ATM), Transmission Electron Microscopy TEM), Electron Backscatter Diffraction (EBSD), and Slow Strain Rate Testing (SSRT) and found that the IGC and SCC susceptibility of the alloy depended strongly on sensitization time and temperature. They also found that the degree of susceptibility to attack for a boundary depended on its crystallographic orientation, with low angle boundaries showing more resistance to attack than their high angle counterparts. Searles et al. [6] studied stress corrosion cracking of AA5083 sensitized at 150 °C for 333 h using electrochemical measurements, Constant Extension Rate Testing (CERT), and transmission electron microscopy (TEM). The degree of β precipitation on grain boundaries as a function of sensitization time and the composition of the precipitates were analyzed using the

I. N. A. Oguocha (✉) · O. J. Adigun
Department of Mechanical Engineering, University of Saskatchewan, 57 Campus Drive, Saskatoon, SK, Canada S7N5A9
e-mail: iko340@mail.usask.ca

S. Yannacopoulos (✉)
School of Engineering, The University of British Columbia Okanagan, 3333 University Way, Kelowna, BC, Canada V1V 1V7
e-mail: spiro.yannacopoulos@ubc.ca

TEM. They concluded that the ductility of the alloy depended strongly on sensitization time. The degradation of the corrosion resistance of AA5083 alloy after thermal and superplastic forming processes was studied by Chang and Chuang [4] using Nitric Acid Mass Loss Test (NAMLT) and electrochemical measurements in 3.5 wt.% NaCl solution. Their results showed that superplastically formed specimens were more susceptible to IGC than the as-received and heat treated specimens. The difference in susceptibility was attributed to sensitization and cavities formed during the superplastic forming process.

Apart from β phase precipitation, segregation of elemental magnesium to grain boundaries during elevated temperature exposure of Al–Mg alloys has also been observed [7–11], but there are conflicting reports about its effect on SCC. For example, Windisch et al. [7] reported that Mg enrichment promoted corrosion of aluminum in 3.5 wt.% salt solution at pH of 10. However, Baer et al. [8] showed through Auger Electron Spectroscopy (AES) and TEM that although alloys with magnesium segregation and Al_3Mg_2 precipitates on the grain boundaries were more susceptible to corrosion cracking, the segregated Mg had little effect on the actual cracking process. This view was supported by a later work by Jones et al. [9] who investigated the role of Mg in the stress corrosion cracking of an AA5083-H321 alloy using AES and Analytical Electron Microscopy (AEM). They found that elemental magnesium that segregated to grain boundaries did not contribute to SCC of the alloy. Crack–particle interactions during intergranular stress corrosion of AA5083-H321 and Al_3Mg_2 were studied by Jones et al. [12] using electrochemical measurements and TEM. Samples solutionized, quenched, and aged for 100 h were tested in both chromate and chromate-free 3.5 wt.% NaCl solution, and the result showed that β phase particles were converted to Al_2O_3 particles on which cracks transversed around.

AA5083 alloy with H116 temper is specially rolled to avoid grain boundary precipitation and hence improve the resistance of standard AA5083 to IGC and SCC [16, 22]. However, in spite of this control, it may still be vulnerable to sensitization when exposed to elevated temperatures for a long time. Therefore, the purpose of the present study was to investigate the effect of sensitization temperature and time on properties (mechanical and chemical) of AA5083-H116. The evaluation methods used included tensile testing, hardness measurements, optical metallography, Scanning Electron Microscopy (SEM), and Energy Dispersive X-ray Spectroscopy (EDS).

Experimental procedure

Aluminum alloy AA5083-H116 plates used in this study were supplied by Alcan Aluminum Limited, Kingston, Ontario, Canada, the chemical composition of which is shown in Table 1. As-received and sensitized samples of the alloy were studied using various techniques in order to understand the effect of sensitization heat treatment on its properties. Test specimens were sensitized by aging at 80, 100, 150, 175, and 200 °C in an air furnace for various lengths of time. Specimens used for hardness measurements, optical metallography, SEM and quantitative EDS analyses were metallurgically polished to high smoothness using 240–600-grit emery papers and 1-μm diamond paste, cleaned with methanol, and dried. The specimens used for optical metallography were further etched by immersing in a warm (60 °C) solution of 10 vol.% H_3PO_4 and 90 vol.% distilled water for 5 min.

The specimens used for studying the IGC susceptibility were prepared in accordance with ASTM G 67 [23]. They were polished with emery cloth, cleaned with methanol, dried, and subsequently sensitized in the same manner as the specimens used for hardness measurements and tensile test. They were later subjected to Nitric Acid Mass Loss Test (NAMLT) following the ASTM G 67 procedure. Susceptibility was measured in terms of mass loss per unit area (mg/cm^2). The mass loss per unit area reported in this work is the average of three tests.

The microstructural features of AA5083-H116 alloy such as intermetallic phases were studied using a JEOL JSM Model 5900 LV SEM equipped with an INCA EDS system. The rectangular specimens used were metallurgically polished using emery papers and 1-μm diamond paste to obtain a high degree of smoothness. All specimens were examined at an acceleration voltage of 20 kV. Figure 1 shows a typical SEM micrograph of AA5083. EDS point analysis of the intermetallic particles labeled A and B in the figure showed that they are Al–Fe–Mn-rich and Mg–Si-rich particles, respectively. Figure 2 shows typical EDS spectra for these particles, while Tables 2 and 3 show representative results of their quantitative EDS analyses.

Hardness measurements were taken using a Buehler Micromet II Vickers Microhardness tester with a load of 200 g applied for 15 s. Two samples were prepared for each test point. Fifteen microhardness readings were taken from each sample to ensure representative result.

Table 1 Chemical composition of AA5083-H116

Element	Cu	Fe	Mg	Mn	Si	Ti	V	Zr	Cr	Al
Wt.%	0.030	0.275	4.942	0.538	0.040	0.004	0.012	0.00	0.091	Rest

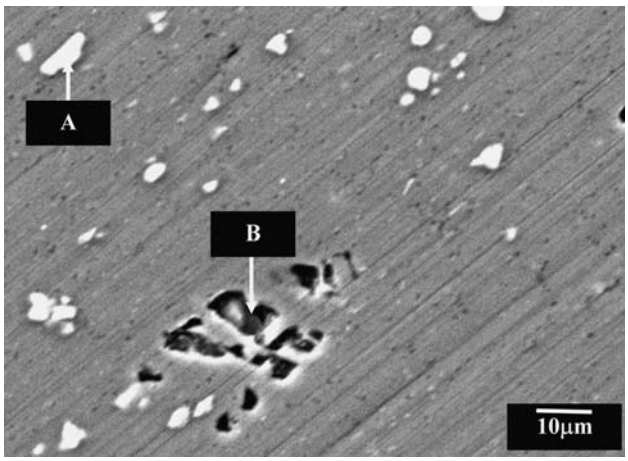

Fig. 1 Typical SEM micrograph of as-received AA5083-H116 showing Al–Fe–Mn-rich particle (arrow A) and Mg–Si-rich particle (arrow B)

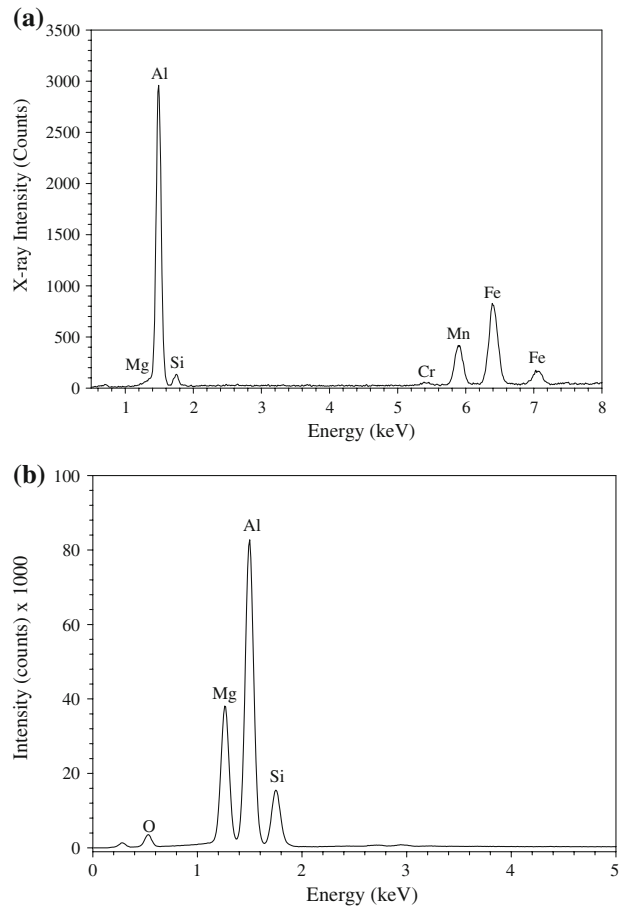

Fig. 2 EDS spectra of (**a**) Al–Fe–Mn rich and (**b**) Mg–Si rich particles shown in Fig. 1

Tensile specimens were prepared from a 9.61-mm-thick plate of the alloy in accordance with ASTM B557M-02a and afterward sensitized in the same manner as those used for hardness measurements. Figure 3 shows the tensile test specimen geometry and dimensions. Tensile testing was carried out using an Instron® Model 1137 tensile machine with an initial strain rate of 0.0033 s^{-1}. Figure 4 shows typical stress–strain curves obtained for the as-received specimen and specimens sensitized at 175 °C for various lengths of time. The tensile and yield strengths reported in this work represent the average of three tests. The fracture surfaces of the tensile specimens were examined in the SEM.

Table 2 EDS point analysis of the Al–Fe–Mn-rich particles

Particle #	Mg	Al	Si	Mn	Fe
1	2.89	79.87	0.08	6.06	11.18
2	2.88	79.35	0.14	6.05	11.16
3	3.28	72.00	1.49	8.56	13.55
4	2.10	65.80	0.09	8.94	23.17

Table 3 EDS point analysis of the Mg–Si-rich particles

Elements (wt.%)				
Particle #	Mg	Al	Si	O
1	18.86	55.37	19.17	6.60
2	26.91	52.41	16.94	3.73
3	17.32	55.35	18.44	8.44
4	12.34	65.11	13.81	8.57

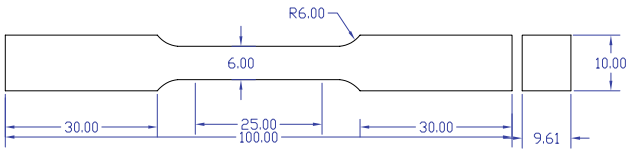

Fig. 3 Tensile test specimen geometry and dimension (mm)

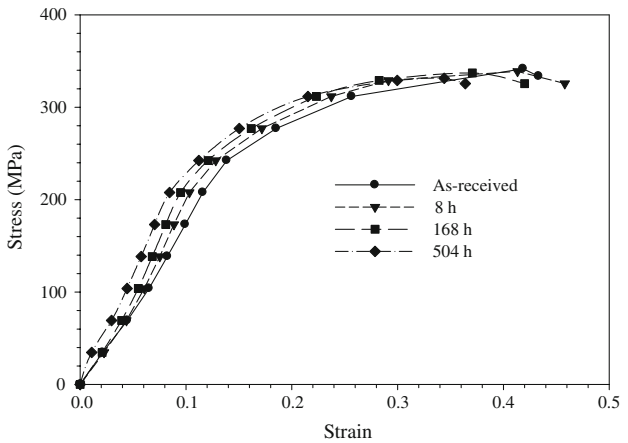

Fig. 4 Typical stress–strain curves for as-received specimen and specimens sensitized at 175 °C

Results and discussion

Metallographic examinations of as-received and sensitized specimens were carried out to better understand the effect of sensitization temperature and time on the grain size and microstructure of AA5083-H116. Figures 5 and 6 are typical optical micrographs obtained for specimens sensitized for 1 week (168 h) at various temperatures and for different lengths of time at 175 °C, respectively. The grain size of specimens sensitized at 200 °C (see Fig. 5) was appreciably smaller than that sensitized at lower temperatures. Also, as shown in Fig. 6, grain size decreased with increasing sensitization time at 175 °C. The difference in grain size is attributed to the extent of recrystallization at each temperature. It can also be seen that specimens sensitized at 175 °C (Fig. 5d) contained more particles within the grains compared to the as-received specimen and specimens sensitized at other temperatures. It is not immediately clear why this happened, but it may be an indication that the temperature at which sensitization of the alloy is maximum is close to 175 °C.

Figure 7 shows the variation in the hardness of AA5083-H116 with sensitization temperature and time, while the variation of its tensile and yield strengths with sensitization temperature and time is shown in Fig. 8. The hardness values, measured in the longitudinal rolling direction, decreased with increasing sensitization temperature and time. The average tensile and yield strengths of the as-received sample were 341 MPa and 248 MPa, respectively, which are slightly greater than 315–317 MPa and 228–230 MPa quoted, respectively, for AA5083-H116 in references [14, 16]. The as-received yield and tensile strengths are greater than those of sensitized samples. Figure 9a and b shows typical SEM micrographs of fracture surfaces obtained for specimens sensitized at 200 °C for168 h (1 week) and 672 h (4 weeks), respectively. The fracture surfaces display a wide range of dimple and cleavage features as well as fracture modes. Dimples initiated at sites where intermetallic particles fractured as well as at interfaces between the matrix and intermetallic particles.

The reduction in hardness and strength with increasing sensitization temperature and time can be attributed partly

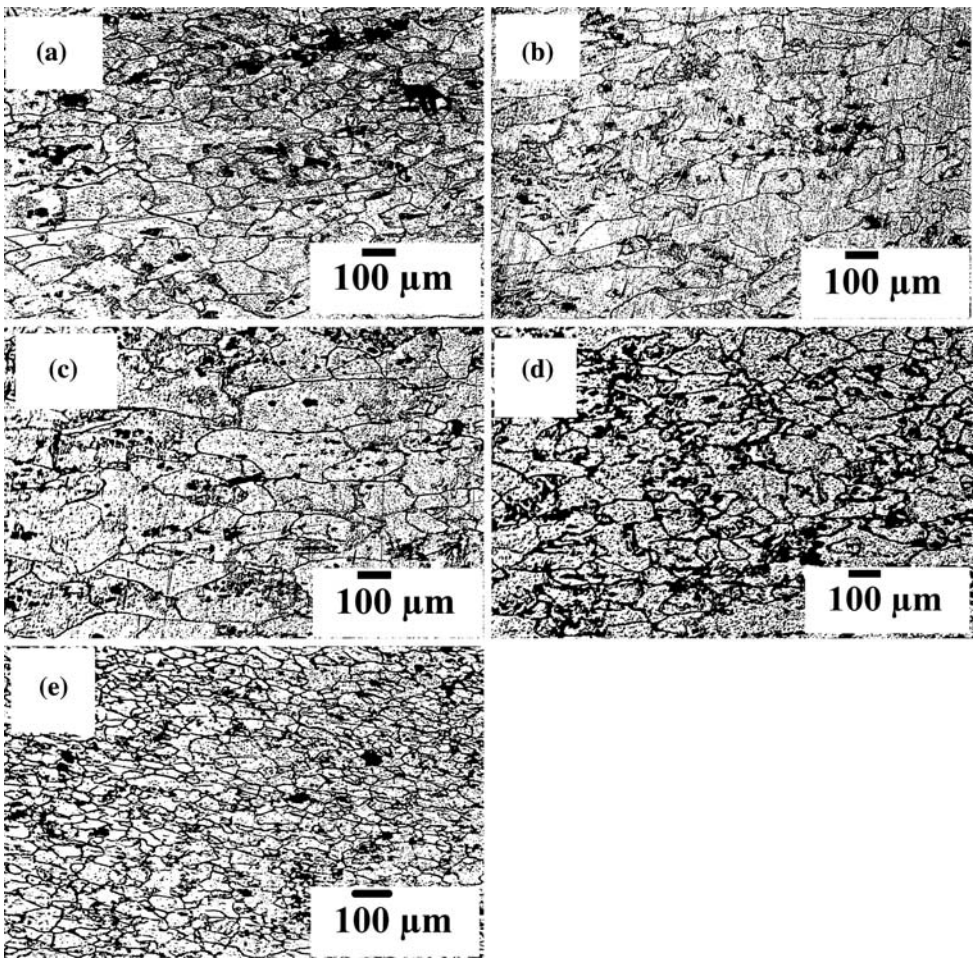

Fig. 5 Optical micrographs showing the effect of sensitization heat treatment on the microstructure of as-received specimen and specimens sensitized at various temperatures for 168 h: (**a**) as-received (**b**) 100 °C, (**c**) 150 °C, (**d**) 175 °C, (**e**) 200 °C

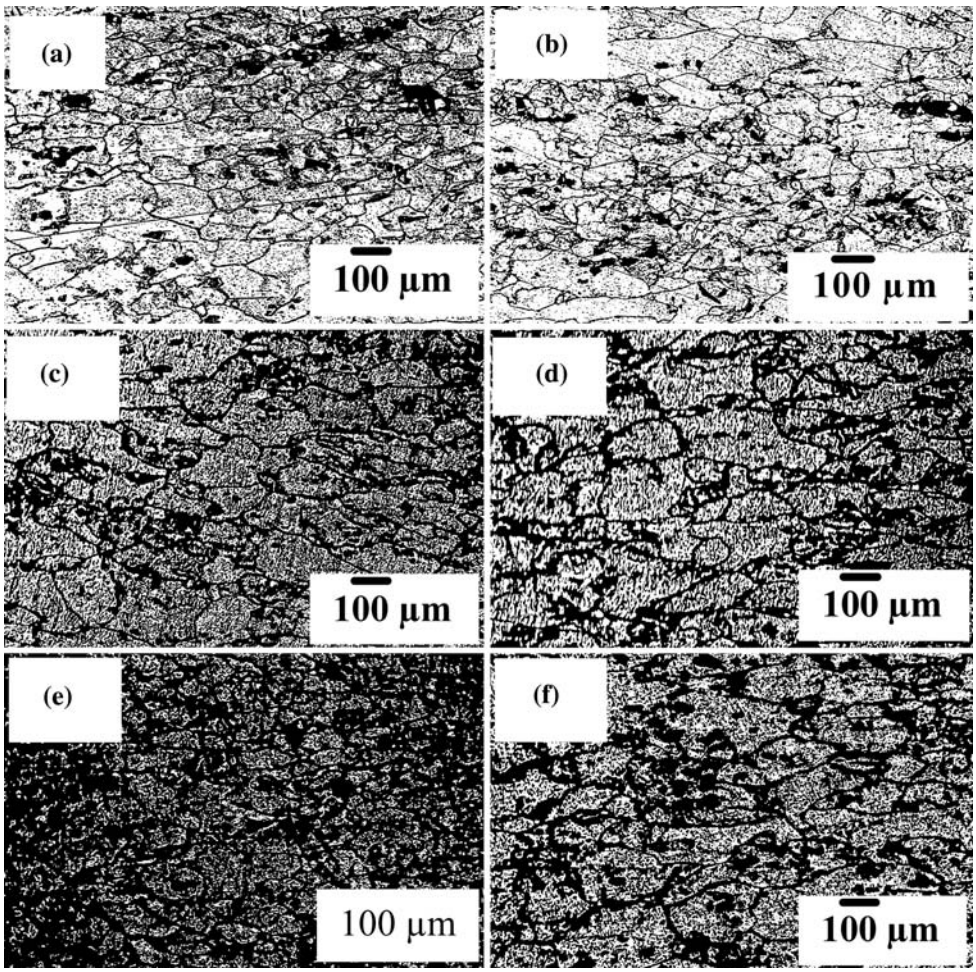

Fig. 6 Optical micrographs showing the effect of sensitization heat treatment on the microstructure of as-received specimen and specimens sensitized at 175 °C for different lengths of time: (**a**) as-received (**b**) 24 h, (**c**) 168 h, (**d**) 336 h, (**e**) 504 h, (**f**) 672 h

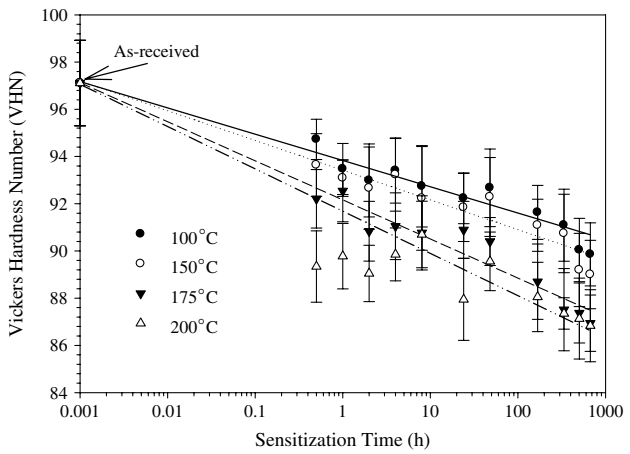

Fig. 7 Variation of hardness with sensitization temperature and time for AA5083-H116

to reduction in the density of dislocations during recrystallization of the cold-worked as-received specimens. It is generally known that the degree of recrystallization in metallic alloys depends on annealing temperature and time. The density of dislocations would therefore decrease as new grains are formed during the sensitization heat treatment. Thus, the hardness, tensile, and yield strengths of the recrystallized structure would be inferior to those of the supplied cold-worked specimens. The formation of strain-free grains as the sensitization temperature and time increased could therefore be responsible for the drastic drop in the tensile and yield strengths of specimens sensitized at elevated temperatures (175 and 200 °C) compared to those sensitized at lower temperatures (100°C and 150°C). The reduction in hardness and strength with increasing sensitization temperature and time can also be attributed to the precipitation of the Mg-rich phase and segregation of Mg atoms at grain boundaries, which draws solute Mg atoms away from the α-matrix. Consequently, as the concentration of solute Mg atoms decreases during sensitization heat treatment, the remaining Mg atoms left behind in solid solution become ineffective obstacles to the movement of dislocations. Further, the grain boundary precipitates cause early fracture of the material during tensile testing [24]. A number of researchers have reported that a decrease in the solute atoms in solid solution could lead to a decrease in mechanical properties [24–26].

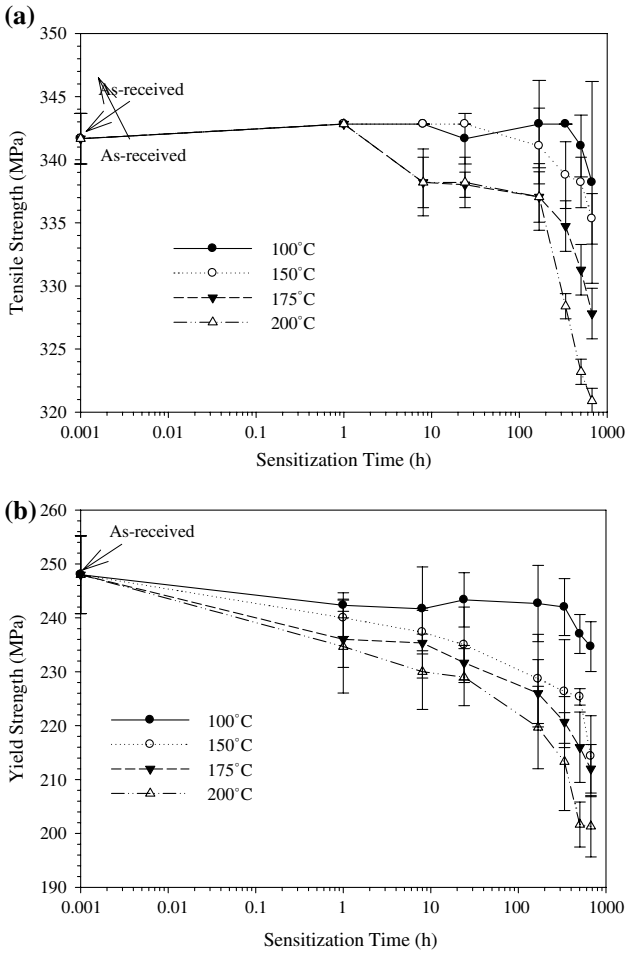

Fig. 8 Effect of sensitization heat treatment on (**a**) tensile strength and (**b**) yield strength of AA5083-H116

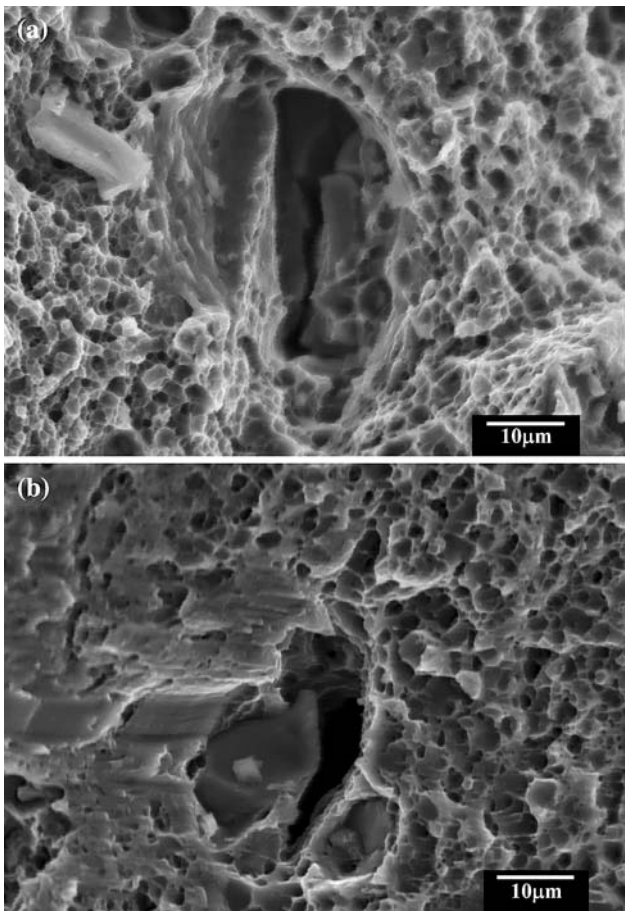

Fig. 9 SEM fractographs of AA5083-H116 specimens sensitized at 200 °C for (**a**) 168 h and (**b**) 672 h

Figure 10 shows the variation of the degree of IGC susceptibility with sensitization heat treatment for the tested AA5083-H116 samples. The data were derived from the nitric acid mass loss test (NAMLT). The minimum aging times required for the alloy to become susceptible to IGC at various temperatures are shown in Fig. 11. From these data, it can be seen that the susceptibility of AA5083-H116 to IGC increased with sensitization temperature and resident time. According to the ASTM G-67 standard [23], a material is considered to be resistant to IGC when the mass loss per unit area it suffers in the NAML test is less than or equal to 15 mg/cm^2. If this loss is greater than or equal to 25 mg/cm^2, then the material is susceptible to IGC. For intermediate mass loss, metallographic examination is required to establish whether or not it is due to intergranular attack. It is important to observe that the susceptibility of AA5083 to IGC at 150 and 175 °C is greater than at 200 °C, thus indicating the existence of a critical sensitization temperature somewhere between 150 and 200 °C where it is maximum. This finding is consistent with the results in reference [14], where it was reported that the temperature where the precipitation rate of the β phase reached a maximum was between 150 and 200 °C. Sampath et al. [5] have also reported that the critical temperature for precipitation of Mg-containing intermetallics in AA5083-O is approximately 150 °C, which is consistent with what had been reported for the precipitation of Mg_5Al_8 in Al–Mg alloys by Perryman and Hadden [19].

Figure 10 also shows that IGC susceptibility for specimens sensitized at 175 °C decreased after 336 h (2 weeks). Van der Hoeven et al. [14] reported that the precipitation rate of the β phase (Al_3Mg_2) decreased when AA5083 is sensitized above 200 °C due to increased solubility of magnesium in aluminum. Beck and Sperry [21] also reported that when random precipitation of Al_3Mg_2 occurs within grains and along the grain boundaries due to heat treatment, susceptibility to both IGC and SCC would be reduced as a result of reduction in the corrosion current density on each anodic region. Therefore, the reduction in susceptibility observed in the present study for specimens sensitized at 175 °C for 336 h and above is believed to be due to precipitation of the β phase within the grains.

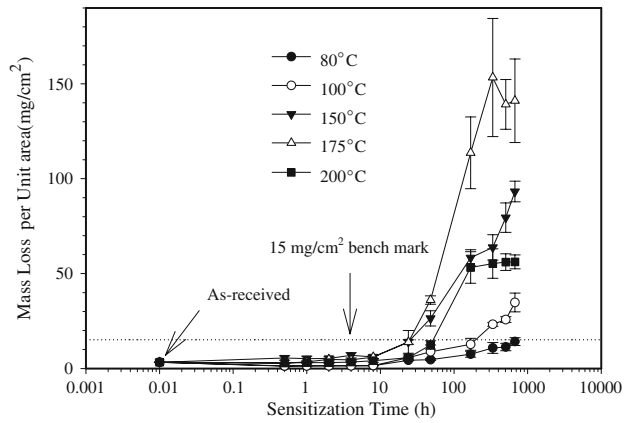

Fig. 10 Effect of sensitization temperature and time on IGC susceptibility of AA5083-H116

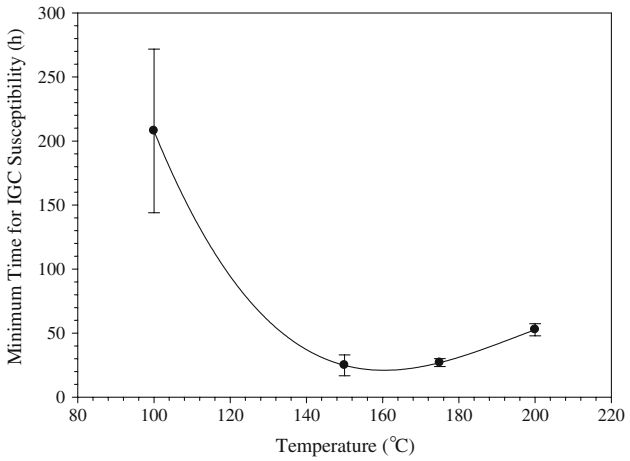

Fig. 11 Minimum sensitization time for AA5083-H116 to become susceptible to IGC at various temperatures

Conclusions

The following conclusions can be drawn from the current work:

1. Specimens of as-rolled AA5083-H116 sensitized at 80 °C up to 672 h are resistant to IGC, but the resistance decreases sharply at higher sensitization temperature and time.
2. Reduction in the hardness and strength of specimens sensitized at elevated temperatures for a long time is due partly to recrystallization and partly to reduction in the concentration of Mg atoms in solid solution.
3. The critical temperature at which AA5083-H116 is most susceptible to IGC lies between 150 and 200 °C.

Acknowledgements The authors would like to thank the Natural Science and Engineering Research Council (NSERC) for Discovery Grants given to Prof. S. Yannacopoulos and Prof. I. N. A. Oguocha and Dr. A. K. Gupta of Alcan Aluminum Limited, Kingston, Ontario, Canada, for supply of test materials and scientific input. We also thank Prof. M. C. Chaturvedi at the University of Manitoba, Winnipeg, for making use of his SEM and EDS facilities.

References

1. Searles JL, Gouma PI, Buchheit RG (2001) Metall Mater Trans A 32:2859
2. Jones RH (1992) In: Stress corrosion cracking. ASM International, Materials Park, Ohio
3. Davenport AL, Yuan Y, Ambat R, Connolly BJ, Strangwood M, Afseth A, Scamans G (2006) Mater Sci Forum 519–521:641
4. Chang JC, Chuang TH (1999) Metall Mater Trans 30A:3191
5. Sampath D, Moldenhauer S, Schipper HR, Mechsner K, Haszler A (2000) Mater Sci Forum 331–337:1089
6. Searles JL, Gouma PI, Buchheit RG (2002) Mater Sci Forum 396–402:1437
7. Windisch CF Jr, Baer DR, Engelhard MH, Danielson MJ, Jones RH (2000) Presented at the 198th meeting of the Electrochem. Soc., Phoenix, AZ
8. Baer DR, Windisch CF Jr, Engelhard MH, Danielson MJ, Jones RH, Vetrano JS (2000) J Vac Sci Technol A 18:131
9. Jones RH, Baer DR, Danielson MJ, Vetrano JS (2001) Metall Mater Trans 32A:1699
10. Vetrano JS, Williford RE, Jones RH (1997) In: Das SK (ed) Automotive alloys I. TMS Annual Meeting. Orlando, FL, TMS Warrendale, PA, p 77
11. Lea C, Molinari C (1984) J Mater Sci 19:2336
12. Jones RH, Gertsman VY, Vetrano JS, Windissch CF Jr (2004) Scripta Mater 50:1355
13. Esposto FJ, Zhang CS, Norton RR, Timsit RS (1994) Surf Sci 302:109
14. Van Der Hoeven JA, Zhuang L, Schepers B, De Smet P, Baekelandt JP (2002) Aluminum 78:750
15. Miller WS, Zhuang L, Bottema J, Witterbrood AJ, De Smet P, Haszler A, Vieregge A (2000) Mater Sci Eng A280:37
16. Hatch JE (1984) In: Aluminum: properties and physical metallurgy. American Society for Metals, Metals Park, Ohio, p 353
17. Davis JR (1999) In: Aluminum and aluminum alloys. ASM Specialty Handbook, Materials Park, OH
18. Chen J, Morris JG (2002) In: A study to reduce age softening of AA5182 aluminum alloy. Research Report for ARCO Aluminum Corp., p 23
19. Perryman WEC, Hadden SE (1950) J Inst Metals 77:207
20. Chang JC, Chuang TH (2002) J Mater Eng Perform 9:253
21. Beck AF, Sperry PR (1969) In: Fundamental aspects of stress corrosion cracking. NACE, Houston, TX, p 513
22. Clausen AH, Borvik T, Hopperstad OS, Benallal A (2004) Mater Sci Eng A364:260
23. Standard Test Method for Determining the Susceptibility to Intergranular Corrosion of 5XXX Series Aluminum Alloys by Mass Loss after Exposure to Nitric Acid (NAMLT Test), ASTM G 67 (2003)
24. Wen W, Zhao Y, Morris JG (2005) Mater Sci Eng A392:136
25. Wen W, Morris JG (2003) Mater Sci Eng A354:279
26. Harun HJ, Mccormick PG (1979) Acta Metall 27:155